

Automatika

Journal for Control, Measurement, Electronics, Computing and Communications



ISSN: (Print) (Online) Journal homepage: www.tandfonline.com/journals/taut20

Performance analysis of triple-band miniaturized hexagonal ultra-wideband antenna for wireless body worn applications

Sesha Vidhya S, Rukmani Devi S, Shanthi K. G & Santhi S

To cite this article: Sesha Vidhya S, Rukmani Devi S, Shanthi K. G & Santhi S (2023) Performance analysis of triple-band miniaturized hexagonal ultra-wideband antenna for wireless body worn applications, *Automatika*, 64:4, 1089-1094, DOI: [10.1080/00051144.2023.2246246](https://doi.org/10.1080/00051144.2023.2246246)

To link to this article: <https://doi.org/10.1080/00051144.2023.2246246>



© 2023 The Author(s). Published by Informa UK Limited, trading as Taylor & Francis Group.



Published online: 18 Aug 2023.



Submit your article to this journal [↗](#)



Article views: 433



View related articles [↗](#)



View Crossmark data [↗](#)



Performance analysis of triple-band miniaturized hexagonal ultra-wideband antenna for wireless body worn applications

Sesha Vidhya S^a, Rukmani Devi S^b, Shanthi K. G^a and Santhi S^c

^aDepartment of Electronics and Communication Engineering, RMK College of Engineering and Technology, Chennai, India; ^bDepartment of Electronics and Communication Engineering, RMD Engineering College, Chennai, India; ^cDepartment of Computer Science Engineering, Kalaigarkaranidhi Institute of Technology, Coimbatore, India

ABSTRACT

The creation of a network of tiny sensors installed in, on or around the human body has been facilitated by advancements in wireless communications and wearable devices. Because of its potential to transform healthcare delivery, Wireless Body Area Network (WBAN) has been increasingly important in modern medical systems over the last decade. Individual nodes (sensors and actuators) embedded in a person's clothing, body, or skin form a WBAN. Both academia and industry have increased their efforts in WBAN research and development. The wearable antenna, whether on or off the human body, is a critical component of contact with particular design in WBAN networks. Ultra-wideband (UWB) technology can provide high-capacity, short-range communications with minimal energy consumption, which is appropriate for wireless body area networks. The human body's involvement in such a device creates significant challenges for both the wearable antenna's construction and the broadcast paradigm. To achieve many functionalities, multi-band and broadband antennas are better solutions. The proposed multi-band antenna is constructed from a FR4 substrate with dimensions of $(24 \times 25 \times 1.6) \text{ mm}^3$. The proposed design was successfully tested with different configurations and enhanced with a broad impedance bandwidth of over 100 percent, where the UWB frequency spectrum encompassed the range from 3 to 9 GHz with a reflective coefficient of -15 dB and gain of 2.5 dBi , as well as fair radiation patterns in the Federal Communications Commission range. The SAR value of the devised antenna with and without SRR being 2 W/kg , 3.5 W/kg , respectively. This solution may be a worthy contender for meeting the UWB demands as a result, could be an excellent fit for wireless body technologies.

ARTICLE HISTORY

Received 29 January 2023
Accepted 3 August 2023

KEYWORDS

WBAN (Wireless body area network); UWB (Ultra-wideband); FCC (Federal communications commission); SRR (Split ring resonator); AMC (Artificial magnetic conductor)

1. Introduction



In recent years, the wireless body area network (WBAN) has attracted a lot of attention and interest due to its numerous uses in health monitoring, military, safety screening, recreation, entertainment, emergency response services and care for underprivileged children and the elderly [1–3]. WBAN is based on the communication link, and can be divided into three categories: in-body, on-body and off-body communications. Aside from in-body communications, there are two types of channels that can be established: on-body (nodes on the body) and off-body (a node on the body interacts with a node outside the body's influence). On-body and off-body modes have different radiation pattern requirements: on-body mode requires a monopole-like omnidirectional radiation pattern, whereas off-body mode requires a broadside radiation pattern [4,5]. Wearable antennas must be low-cost, light-weight and almost maintenance-free in order to be useful in contemporary applications. Wearable antennas, as a result, play an important role in wireless on-body centric

communications and are generating a lot of research attention [6,7].

WBANs can be used in medical applications to continuously monitor physiological parameters like as blood pressure, heart rate and body temperature. Data acquired by the sensors can be communicated to a gateway, such as a mobile phone, if abnormal conditions are identified. The gateway then sends its data to a remote location, such as an emergency department or a doctor's office, over a cellphone network or the Internet, so that action can be performed [8,9].

The antenna radiation pattern and antenna sensitivity to the human body are two important needs for on-body antenna communication. Loop antennas, patch antennas, patch array antennas and monopole antennas have all been conceived and built for use in the 2.5 GHz and ISM bands. The monopole and monopole combinations, in particular, have the lowest link loss and the largest path gain [10].

In a WBAN network, ultra-wideband (UWB) technology is a good choice for reducing the power

CONTACT Sesha Vidhya S  sesha.puru@gmail.com  Associate Professor, Department of Electronics and Communication Engineering, RMK College of Engineering and Technology, Chennai, India

spectrum range, which means longer battery life and lower electromagnetic sensitivity for persistent on-body operation [11,12].

The planar monopole antenna topology is widely used in UWB communication systems and is considered as the first topology utilized in wearable applications due to its ease of construction, broad bandwidth and good radiation efficiency. The rapid growth of wireless networking technologies has necessitated continual antenna design improvements. Particularly after the FCC allocated the frequency spectrum from 3.1 GHz to 10.6 GHz for usage without a licence in February 2002. Federal Communications Commission [13].

Because WBAN devices use wearable antennas for on-body contact, the radiation pattern in the horizontal plane must be omnidirectional and the orientation for the human site must be longitudinal. As a result, a vertical monopole with a large field is an excellent choice for these designs. Nonetheless, the height should be reduced greatly and the bandwidth should be enhanced to match the intended uses, in order to preserve practicality [14].

2. Background

For WBAN, Yang et al. [15] presented a low-profile UWB antenna with a metalized ground plate made up of FR-4 substrate with a thickness of 1 mm and a metalized ground plate made of copper measuring (80×80) mm². This antenna combines the advantages of both monotone and printed antennas, resulting in a design that is inexpensive in weight, easy to fabricate and offers wideband and omnidirectional radiation patterns. For a frequency range of 2.5–24 GHz. As a result, the human body's influence on the suggested antenna was minimal, and the low-profile UWB antenna's time-domain activity was examined.

Bhanumathi and Swathi [16] also designed and built a small microstrip antenna with a FR4 as substrate, overall dimensions of (24×36) mm². Based on the signal interference concept, an antenna with a dual-feed line construction was designed to reduce the un-radiating terminal. Furthermore, the antenna functioned in the 4.8–7.8 GHz frequency spectrum, making it an excellent choice for UWB applications.

Danjuma et al. [17] also introduced a small rectangular slot antenna that is essential for centric applications of the ultra-wideband body. The antenna is made on an FR4 substrate with dimensions of (dielectric constant $\epsilon = 4.3$, loss tangent $\delta = 0.025$ and thickness $h = 0.8$ mm) and an overall antenna size of (14.9×33.12) mm². Because of the comparability established between ON and OFF body measurements, the antenna was a solid candidate for focal applications in wireless body technologies.

Tan et al. [18] developed a miniaturized planar UWB slot antenna with dual-polarization MIMO with overall antenna dimensions of (32×22) mm² manufactured on a low-cost FR4-epoxy substrate with $\epsilon = 4.6$, $\delta = 0.02$ and $h = 0.8$ mm and a frequency range of 3.05–10.61 GHz for UWB applications.

Toktas and Yerlikaya [19] also show a tiny printed monopole antenna in the UWB G-shaped type was built on a low-cost double copper-sided FR4 epoxy substrate with $\epsilon = 4.4$, $\delta = 0.017$ and $h = 1.6$ mm in a compact dimension of (8×27.5) mm² to operate in the frequency range 2.8–12.6 GHz.

Joshi and Singhal [20] describe a UWB antenna with hexagonal patch vertices. Over a (46×46) mm² FR-4 substrate, a circumradius hexagonal patch, $R = 16.5$ mm and a circumradius concentrate hexagonal slot, $r_{\text{cut}} = 3$ mm are developed. For impedance bandwidth and WLAN band rejection, the prototype antenna achieved (8.3) GHz from 2.3 to 10.6 GHz and (1.6) GHz from 4.9 to 6.5 GHz, respectively. The antenna calculations show that removing the flange turns a C-band antenna into a UWB antenna.

The aforementioned UWB antennas were built for body area network applications, and the majority of the antennas were very big, with little analysis of surface current distribution. In wearable antenna applications, the size, impedance bandwidth and radiation characteristics of the antenna play a critical role. With Artificial Magnetic Conductor (AMC) material Split ring Resonator (SRR), we presented a multiband small UWB antenna. The difficulty of delivering wide bandwidth, small size and low backward radiations for a viable on-body application is solved.

The study is organized as follows: the third portion describes the material utilized, as well as the antenna's design and different structure analysis; the fourth section includes simulated findings in terms of antenna parameters, which have been compared to tested results. Finally, in the fifth portion, the conclusion is delivered.

3. Antenna design

The hexagon-shaped antenna is designed and analysed for performance improvement using FR4 as the substrate and a microstrip line as the feed. The antenna geometry with and without the SRR structure is shown in the diagram below. This antenna is designed to be operated at multi frequencies in the range from 3 to 9 GHz. The suggested antenna is a hexagonal-shaped monopole antenna printed on FR4 substrate ($\epsilon = 4.4$, $\delta = 0.02$) with partial ground and two SRR rings on the ground plane. The antenna structure is very small, with a surface area of 24×25 mm² and a thickness of 1.6 mm. There are two antenna geometry configurations: one without a split ring resonator (SRR) and another one with SRR as shown in Figure 1(a,b).

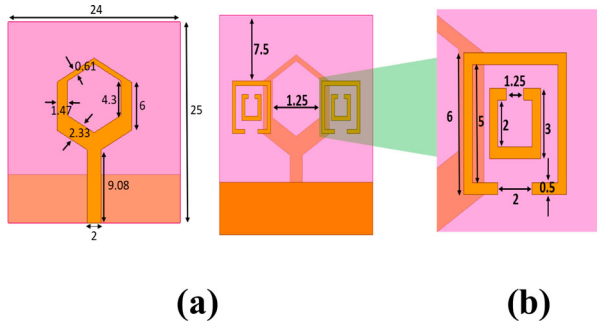


Figure 1. Antenna Geometry (a) without SRR structure (b) with SRR structure.

The formulas to design an antenna for a single frequency. The following formulas will obtain those dimensions; the following are used formulas to develop an antenna for a single frequency.

$$\text{Width, } W = \frac{c}{2f_r \sqrt{\frac{\epsilon_r + 1}{2}}}, \quad (1)$$

where W is the width of the antenna, c is the speed of light, f is the frequency and ϵ_r is the relative permittivity of the substrate or dielectric constant.

$$\epsilon_{\text{reff}} = \frac{\epsilon_r + 1}{2} + \frac{\epsilon_r - 1}{2} \left[1 + 12 \frac{h}{W} \right]^{-1/2}, \quad (2)$$

where ϵ_{reff} are effective permittivity and the height of the substrate.

$$\frac{\Delta L}{h} = 0.412 \frac{(\epsilon_{\text{reff}} + 0.3) \left(\frac{W}{h} + 0.264 \right)}{(\epsilon_{\text{reff}} - 0.258) \left(\frac{W}{h} + 0.8 \right)}, \quad (3)$$

$$\text{Length, } L = L_{\text{eff}} - 2\Delta L, \quad (4)$$

$$L = \frac{\lambda}{2} - 2\Delta L, \quad (5)$$

$$\lambda = \frac{c}{f \sqrt{\epsilon_{\text{reff}}}}, \quad (6)$$

where L_{eff} is the effective length of the patch.

The evolution process of the antenna is employed in order to achieve good impedance matching and reflection coefficient. As the first step, a hexagon-shaped construction with partial ground is printed on FR4 substrate. A microstrip transmission line with a diameter of $2 \times 9.08 \text{ mm}^2$ stimulates the antenna created in step one. Because of the higher inductive reactance caused by the hexagon structure, no impedance matching is achieved, as seen by the reflection coefficient curve of step one in Figure 2. To cancel out this reactance and attempt impedance matching, a step two inner hexagon construction that narrows inward has been used, without affecting the feeding arrangement or compactness. Step two has little contribution to gain impedance matching by cancelling inductive reactance, as seen by the reflection coefficient curve shown in Figure 2 of step two. As a result, without interfering with step two,

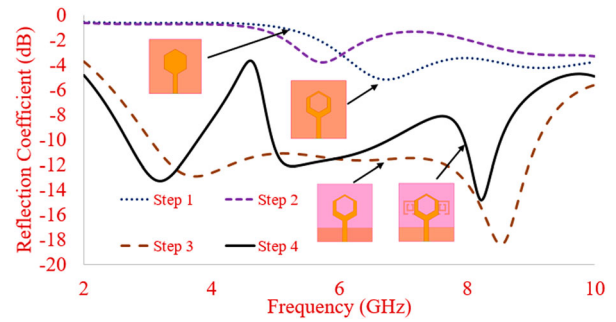


Figure 2. Step-wise evolution process and their reflection coefficient curves using AMC material with SRR.

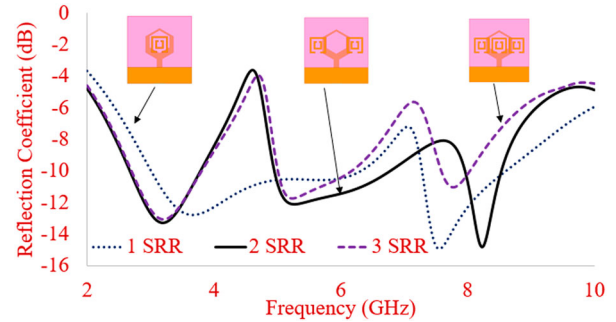


Figure 3. The effect of the number of SRR rings on the proposed small UWB antenna's estimated reflection coefficient using AMC structure.

step three is developed simply by narrowing the inner hexagon slot in an upward direction. In addition, two SRRs were deployed to the right and left sides of the antenna built in steps three and in step four. The reflection coefficient curve as in Figure 2 shows that there is good impedance matching throughout the working region.

A parametric analysis with single, double and triple SRR rings is carried out in order to examine and decide on the right count of SRR rings. The simulated reflection coefficient curve analysis show in Figure 3 that when a single SRR is deployed, impedance matching is not achieved in the desired of interest, whereas when three SRR rings are deployed, the reflection coefficient curve is closer to the proposed antenna's reflection coefficient but with a narrow band range. As can be seen in Figure 3, positioning two SRR rings on the right and left sides of the hexagon helps to achieve the necessary multi-frequency bands of interest.

4. Results and discussion

HFSS is used to model the radio frequency (RF) and radiation performance of the proposed small UWB antenna made of AMC with SRR.

4.1. Reflection coefficient characteristics

Figure 4 shows the HFSS simulated reflection coefficient curves of the proposed UWB antenna employing AMC with SRR and without SRR. The compact UWB

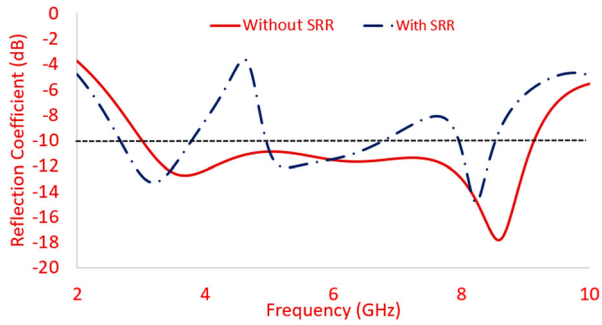


Figure 4. Simulated output of the proposed UWB antenna's reflection coefficient curves using AMC material with and without SRR.

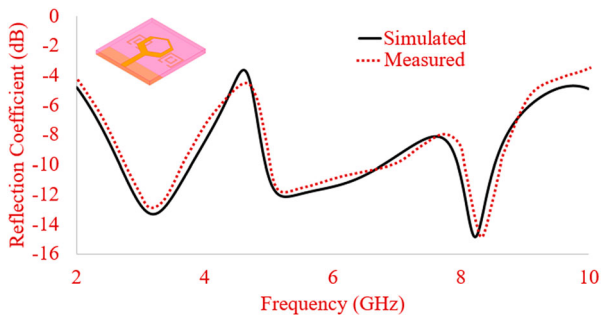


Figure 5. The suggested small UWB antenna's simulated and measured reflection coefficient.

antenna without SRR exhibits impedance bandwidths of 17%, 31% and 7% in the frequency ranges of (2.6–3.8) GHz, (5–6.8) GHz and (8–8.5) GHz, respectively, while a proposed antenna with SRR exhibits impedance bandwidths of 100% in the frequency range of (3–9) GHz.

Figure 5 shows the predicted and measured reflection coefficient of the proposed compact UWB antenna utilizing AMC with SRR. It can be shown that the predicted and measured reflection coefficients curves of the proposed small UWB antenna employing AMC material with SRR agree extremely well.

4.2. Gain

Figure 6 shows the simulated achieved gain performance of the proposed antenna utilizing AMC material with and without SRR. As can be seen in Figure 6, the addition of SRR reduces total bandwidth, but the gain is greatly increased due to the reduction in back radiation. Due to SRR on the ground plane, the gain is more than 2 dBi across the whole range.

Figure 7 shows the simulated and measured realized gain performance of the proposed antenna utilizing AMC material with SRR. It shows that both results are in good agreement with one other, with just minor differences. For smooth operation of the proposed tiny UWB antenna, both simulated and measured results show a gain larger than 2 dBi over the whole range.

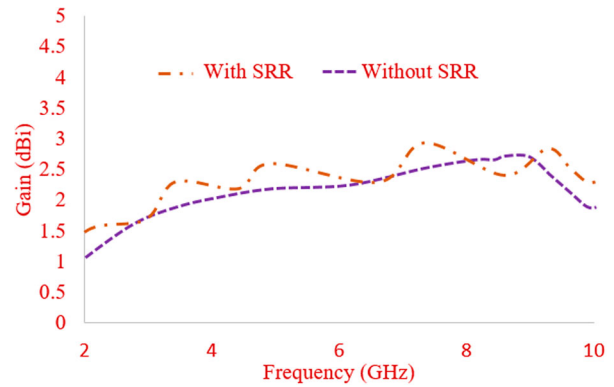


Figure 6. Simulated output of the proposed UWB antenna's gain with and without SRR.

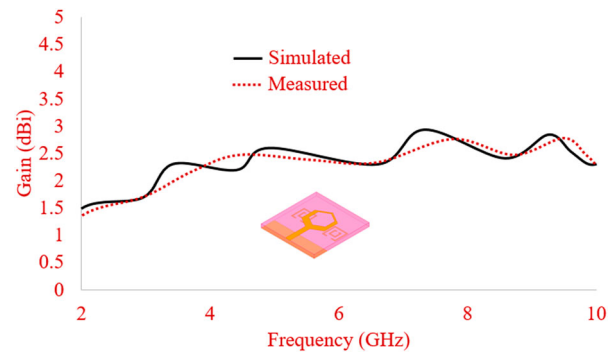


Figure 7. Measured and Simulated gain of the proposed antenna with SRR.

4.3. Surface current (A/m) distribution

Figure 8 shows the simulated surface current distribution of the proposed UWB antenna employing an AMC conductor without and with SRR at 3.6 GHz.

The highest component of current lies on the lower half of the radiating hexagon at 3.6 GHz, as shown in the analysis (Figure 8(a)). Figure 8(b) shows that at 3.6 GHz, the majority of current flows via the upper half of the hexagon as well as the outside SRR. This adds to the emergence of a broad frequency range spanning (2.6–3.8) GHz.

At resonance 6 GHz, as shown in Figure 9(a), the largest amount of current flows through the upper half

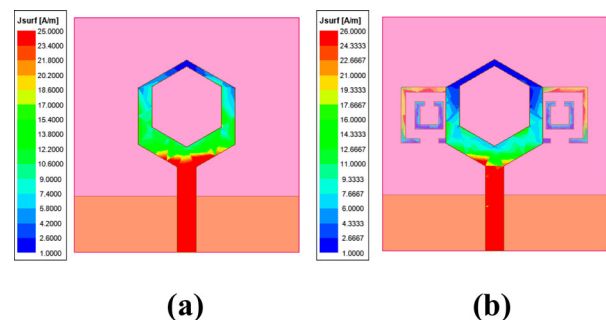


Figure 8. Surface current (A/m) distribution at 3.6 GHz (a) Without SRR (b) With SRR.

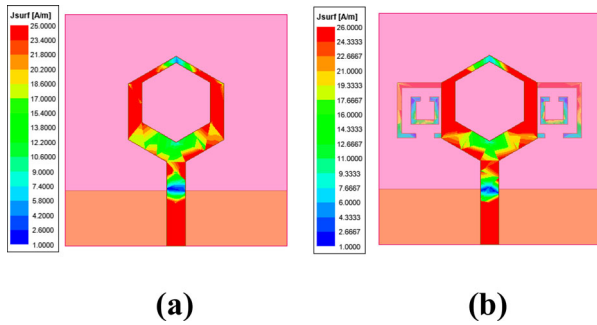


Figure 9. Surface current (A/m) distribution at 6 GHz (a) Without SRR (b) With SRR.

of the hexagon, Figure 9(b) shows that a larger quantity of current flows through the entire hexagon structure as well as the outer ring of the SRR, contributing to the induction of a band of (5–6.8) GHz.

At 8 GHz, the entire hexagon structure allows the maximum current to flow. As a result of the study in Figure 10, it is obvious that the single hexagon radiating structure generates three large resonances spanning a wide band of frequencies ranging from 3 to 9 GHz,

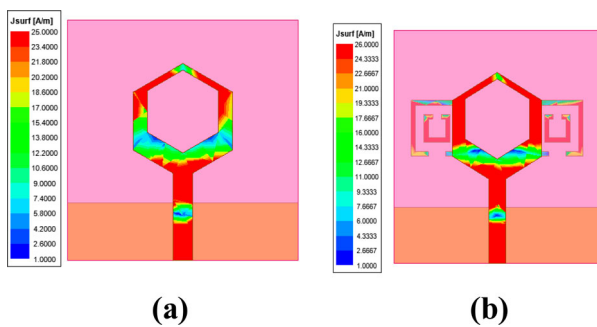


Figure 10. Surface current (A/m) distribution at 8 GHz (a) Without SRR (b) With SRR.

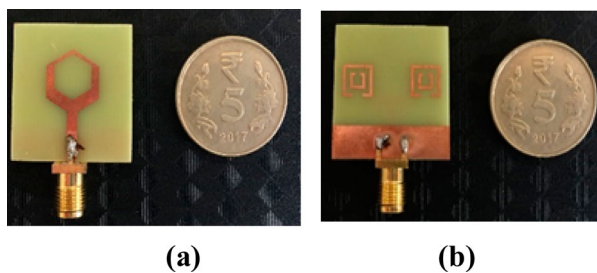


Figure 11. Fabricated prototype of the proposed UWB antenna (a) top view (b) back view.

making the suggested antenna ideal for on-body wearable wireless applications.

The antenna prototype was manufactured and tested as indicated in Figure 11 to validate the performance of the proposed small UWB antenna employing AMC material with SRR. Figure 11(a,b) shows the top and back view of fabricated proposed antenna respectively.

The proposed small antenna's performance is compared to that of existing antenna designs. The performance of several antennas built with the same FR4 substrate is shown in Table 1 with regard to the following parameters: antenna size, Impedance Bandwidth, gain and operating frequency.

As compared to other antennas, the proposed antenna is the smallest and has all of the essential parametric performance, making it the perfect choice for wearable applications.

5. Conclusion

A unique, low-profile, compact hexagonal-shaped monopole with partial ground plane and two SRR rings has been successfully investigated. The suggested antenna has a volume of $24 \times 25 \times 1.6 \text{ mm}^3$, which allows for two configurations (hexagon antenna with and without SRR). With the SRR arrangement, a multi-band impedance bandwidth of 100% (3–9 GHz) is attained, ensuring the usability of the proposed antenna for on-body wearable antenna applications. Furthermore, throughout the working bands, the dipole radiation patterns and gain larger than 2.5dBi support the suitability for smooth wireless data transmission of the human body.

Disclosure statement

No potential conflict of interest was reported by the author(s).

ORCID

Sesha Vidhya S <http://orcid.org/0000-0002-4723-0749>

Rukmani Devi S <http://orcid.org/0000-0002-0153-6283>

Shanthy K. G <http://orcid.org/0000-0001-5201-0903>

References

- [1] Hall PS, Hao Y. Antennas and propagation for body-centric wireless communications. Norwood (MA): Artech House; 2006.

Table 1. Proposed compact UWB antenna performance vs. existing antenna designs.

| Reference | Dimensions (mm ³) | Operating band (GHz) | Impedance bandwidth (%) | Substrate | Gain (dBi) |
|--|-------------------------------|----------------------|-------------------------|-----------|------------|
| M. Mustaqim et al. [21] | 31 × 42 × 1.6 | 3.0–11 | 98 | FR-4 | 4.3 |
| Joshi and Singhal et al. [20] | 46 × 46 × 1.6 | 2.3–10.6 | 88 | FR-4 | 6 |
| A. Toktas and M. Yerlikaya et al. [19] | 8 × 27.5 × 1.6 | 2.8–12.6 | 97 | FR-4 | – |
| M. T. Tan et al. [18] | 32 × 22 × 0.8 | 3.05–10.61 | 123 | FR-4 | 5.74 |
| I. M. Danjuma et al. [17] | 33.12 × 14.9 × 0.8 | 3–10 | – | FR-4 | – |
| V. Bhanumathi and Swathi [16] | 24 × 36 × 1.6 | 4.8–7.8 | 48 | FR-4 | – |
| Yang J. et al. [15] | 80 × 80 × 1 | 2.5–24 | 162 | FR-4 | 10 |
| Proposed antenna | 24 × 25 × 1.6 | 3.02–9.13 | 100 | FR-4 | 3 |

- [2] Seshu Vidhya S, Rukmani Devi S, Shanthi KG. Design trends in ultra wide band wearable antennas for wireless On-body networks. *ARPN J Eng Appl Sci.* 2017;12(9):2782–2790.
- [3] Hall PS, Hao Y. *Antennas and propagation for body-centric wireless communications.* Norwood (MA): Artech House; 2012.
- [4] Pellegrini A, Brizzi A, Zhang L, et al. Antennas and propagation for body-centric wireless communications at millimeter-wave frequencies: a review [wireless corner]. *IEEE Antennas Propag Mag.* 2013;55(4):262–287.
- [5] Werner DH, Jiang ZH, Eds. *Electromagnetics of body area networks: antennas, propagation and RF systems.* Piscataway (NJ): IEEE Press; 2016.
- [6] Abbasi QH, Rehman MU, Qarage K, Eds., et al. 2016. *Advances in body-centric wireless communication: applications and state-of-the art.* Stevenage: IET Press; 2016.
- [7] Hall PS, Hao Y, Eds. *Antennas and propagation for body-centric wireless communications.* 2nd ed. Norwood (MA): Artech House; 2012.
- [8] Xing J, Zhu Y. “Analysis of multi-user detection of multi-rate transmissions in multi-cellular CDMA,” in 5th Int. Conf. on Wireless Communications, Networking and Mobile Computing (WiCom ‘9), pp. 1–20, 2009. doi:10.1002/wcm.671
- [9] Wang B, Pei Y. “Body area networks,” *Encyclopedia of wireless and mobile communications*, edited by Borko Furht, Taylor and Francis, vol. 98, 2007.
- [10] Kamarudin M, Nechayev Y, Hall P. Performance of antennas in the on-body environment. *IEEE Antennas Propag Soc Intl Symp.* 2005;3A:475–478. doi:10.1109/APS.2005.1552290
- [11] Adamiuk G, Zwick T, Wiesbeck W. UWB antennas for communication systems. *Proc IEEE.* 2012;100(7):2308–2321. doi:10.1109/JPROC.2012.2188369
- [12] Schantz HG. Introduction to ultra-wideband antennas. *Proc IEEE Conf Ultra Wideband Syst Technol.* 2003: 1–9. doi:10.1109/UWBST.2003.1267792
- [13] “Revision of part 15 of the commission’s rules regarding ultra-wideband transmission systems,” *Tech. Rep. FCC 02. V48*, Federal Communication. Commission, Washington, DC, USA, 2002.
- [14] Mahmood SN, Ishak AJ, Ismail A, et al. ON-OFF body ultra-wideband (UWB) antenna for wireless body area networks (WBAN): A review. *IEEE Access.* 2020;8:150844–150863. doi:10.1109/ACCESS.2020.3015423
- [15] Yang X, Hu J, Liu S. A low profile UWB antenna for WBAN applications. *IEEE Access.* 2018;6:25214–25219. doi:10.1109/ACCESS.2018.2819163
- [16] Bhanumathi V, Swathi S. Bandwidth enhanced microstrip patch antenna for UWB applications. *ICTACT J Microelectron.* 2019;4(4):669–675. doi:10.21917/ijme.2019.01116
- [17] Danjuma IM, Akinsolu MO, Mohammad B, et al. A compact size and low profile rectangular slot monopole antenna for UWB body centric applications. *Proc USNC-URSI Radio Sci Meeting (Joint with AP-S Symp).* 2019: 91–92. doi:10.1109/USNC-URSI.2019.8861713
- [18] Tan MT, Li X, Wei WH, et al. A planar miniaturized UWB dual-polarization multiple-input-multiple-output slot antenna. *Microwave Optical Technol Lett.* 2020;62(1):432–438. doi:10.1109/USNC-URSI.2019.8861713
- [19] Toktas A, Yerlikaya M. A compact reconfigurable ultra-wideband G-shaped printed antenna with band-notched characteristic. *Microwave Optical Technol Lett.* 2019;61(1):245–250. doi:10.1002/mop.31516
- [20] Joshi A, Singhal R. Probe-fed hexagonal ultra wideband antenna using flangeless SMA connector. *Wireless Personal Commun.* 2020;110(2):973–982. doi:10.1007/s11277-019-06768-2.
- [21] Mustaqim M, Bilal A, Khawaja HT, et al. Ultra-wideband antenna for wearable Internet of Things devices and wireless body area network applications. *Int J Numer Model: Electron Netw Devices Fields.* 2019;32(6):e2590.